

Rigorous Screened Interactions for Realistic Correlated Electron Systems

Charles J. C. Scott^{✉*} and George H. Booth^{✉†}

Department of Physics, King's College London, Strand, London WC2R 2LS, United Kingdom

 (Received 25 July 2023; revised 5 December 2023; accepted 19 January 2024; published 16 February 2024)

We derive a widely applicable first-principles approach for determining two-body, static effective interactions for low-energy Hamiltonians with quantitative accuracy. The algebraic construction rigorously conserves all instantaneous two-point correlation functions in a chosen model space at the level of the random phase approximation, improving upon the traditional uncontrolled static approximations. Applied to screened interactions within a quantum embedding framework, we demonstrate these faithfully describe the relaxation of local subspaces via downfolding high-energy physics in molecular systems, as well as enabling a systematically improvable description of the long-range plasmonic contributions in extended graphene.

DOI: [10.1103/PhysRevLett.132.076401](https://doi.org/10.1103/PhysRevLett.132.076401)

Building effective models that retain the physics of interest but strip away extraneous complexity is central to progress in understanding physical mechanisms and emergent behavior in complex systems. Nowhere is this more true than interacting electron systems, where effective Hamiltonians occupy a central position in both condensed matter and quantum chemistry, from the Hubbard model to ligand field theory [1–4]. A push is now underway to erode the boundary between phenomenological effective models with empirical parameters, and *ab initio* modeling with material specificity, where the act of constructing a *material-specific* effective Hamiltonian is increasingly the first step in a larger workflow involving its subsequent solution within a multimethod approach. This is critical to extend the scope of accurate yet computationally demanding many-body methods, placing significant urgency on approaches in which the relevant physics outside a low-energy model space is rigorously downfolded or renormalized into the effective Hamiltonian [5–7]. In this work we propose a simple and efficient approach to effective interactions, demonstrating quantitative accuracy and specificity resulting from integrating out *ab initio* high-energy and long-range physics, motivated by the exact conservation of instantaneous expectation values.

A salient example in the need for accurate renormalized interactions is quantum embedding, describing correlated many-body phenomena within a local subspace [8–11]. The missing interactions with states outside the subspace

should renormalize the effective subspace interactions in real materials, generally necessitating the use of effective interactions that are often parametrized empirically via Hubbard or Hund terms [12–14], or downfolded from other theories [11,15–17]. In quantum chemistry, analogous subspaces are often described by a “complete active space” (CAS), whereby a small number of low-energy mean-field orbitals are chosen for an accurate treatment of the strong correlation in “multireference” approaches [18]. More broadly, a wide range of both qualitative and quantitative studies into correlated materials rely on first obtaining appropriately screened effective interactions of a simplified model from an *ab initio* starting point [5,19].

It is often argued that the random phase approximation (RPA) contains much of the physics missing from low-energy models, and is the appropriate theory in which to construct effective interactions [11,13,20,21]. As an infinite resummation of the bubble diagrams, it correctly describes the long-range charge fluctuations, plasmons, high-energy scattering, and many-body dispersion that predominates in high-density metallic and semiconducting extended systems [22–24]. While its traditional formulation lacks exchange or ladder diagrams, their contributions generally decay more rapidly and can often be captured within the model space, with approaches to screen beyond RPA still an active research area [15,16,25].

The *constrained* RPA (cRPA) method has therefore become a widespread choice for deriving low-energy effective interactions from first-principles, applied from molecules to Mott insulators and routinely as a precursor to quantum embedding methods [5,8,13,16,25–41]. Since the RPA is a well-defined diagrammatic theory, the bubbles corresponding to the polarizability *within* the model space [$\Pi_m(\omega)$] can be removed from the total polarization [$\Pi_{\text{ext}}(\omega) = \Pi(\omega) - \Pi_m(\omega)$]. The screened interactions, $\mathcal{U}(\omega)$, are then found from the infinite RPA resummation

Published by the American Physical Society under the terms of the [Creative Commons Attribution 4.0 International license](https://creativecommons.org/licenses/by/4.0/). Further distribution of this work must maintain attribution to the author(s) and the published article's title, journal citation, and DOI.

coupling this space to the external degrees of freedom via this scattering channel, as

$$\mathcal{U}(\omega) = v + v\Pi_{\text{ext}}(\omega)v + v\Pi_{\text{ext}}(\omega)v\Pi_{\text{ext}}(\omega)v + \dots, \quad (1)$$

where v denotes the bare Coulomb interaction. In this way, double counting of correlated effects are avoided once the resulting effective model is solved, yet direct scattering events to all orders between the two spaces are included [26]. The cRPA approach is also internally consistent: an RPA calculation on the resulting effective Hamiltonian with interactions $\mathcal{U}(\omega)$, will give exactly the results of the RPA on the full system. More specifically, the cRPA ensures that the RPA density-density (dd) response function, $\chi(\omega)$, of the model space with effective interactions $\mathcal{U}(\omega)$, is identical to the projection of the RPA full system dd response into the model space. In this way, the effective interactions can also be seen to be “state universal,” providing the correctly renormalized interactions for the entire RPA spectrum of the model subspace.

While this puts the cRPA approach on a solid footing, few methods are computationally tractable with the resulting *dynamical* interactions of Eq. (1). Practical necessity therefore forces the widespread approximation of taking the static, $\omega \rightarrow 0$ limit of the screened interaction of Eq. (1) (static-cRPA). This uncontrolled approximation is qualitatively justified in capturing the relevant long-wavelength behavior where the RPA is accurate [25], however forces us to entirely give up on rigorous conservation of any expectation values from the RPA. There is significant skepticism of its accuracy, with the cRPA interactions often overscreening the physics [15,16,25,28,42]. Far from purely a small quantitative shift, this can result in wrong energy ordering of states and phases in the resulting model, or missing spectral weight transfer to plasmon satellites [14,35,43].

A further serious technical limitation of the cRPA approach is that the model space must be chosen from a selection of low-energy bands, rather than directly as local degrees of freedom. Specifically, it requires the irreducible polarizability (defined by the reference mean field) to have no coupling between excitations within the model space and ones in the rest of the system, otherwise $\mathcal{U}(\omega)$ alone is not sufficient to reproduce $\chi(\omega)$. Effective local interactions are therefore found via localization *after* determining the screening of these low-energy bands. However, this is problematic, missing out on screening within the low-energy bands themselves if the resulting local interactions are subsequently truncated (e.g., to the Hubbard or Hund form), and causing further difficulties when it is not possible to fully represent the relevant subspace (e.g., atomic d shells) in the low energy bands due to significant hybridization with other states [29,44]. In addition, the

resulting cRPA screened interactions modify the reference mean-field state, resulting in unintended changes to the subspace density and band structure [28,42,45].

To motivate our approach, we ask an alternative pertinent question: What physical quantities *can* we rigorously conserve at the RPA level in a chosen model space, under the constraint that the resulting effective interactions must remain *static* and *two-body*? This leads to the development of the “moment-constrained” RPA (mRPA) approach, which exactly conserves the *instantaneous* part of the two-point dd response in the model subspace, as well as the reference state. We argue that conserving physical expectation values in the construction of effective static interactions provides a more rigorous foundation than the widespread static-cRPA approximations.

Moment-constrained RPA.—The RPA can be formulated as a quasibosonic eigenvalue problem in the space of particle-hole excitations and deexcitations of a reference state [46],

$$\begin{bmatrix} \mathbf{A} & \mathbf{B} \\ -\mathbf{B} & -\mathbf{A} \end{bmatrix} \begin{bmatrix} \mathbf{X} & \mathbf{Y} \\ \mathbf{Y} & \mathbf{X} \end{bmatrix} = \begin{bmatrix} \mathbf{X} & \mathbf{Y} \\ \mathbf{Y} & \mathbf{X} \end{bmatrix} \begin{bmatrix} \boldsymbol{\Omega} & \mathbf{0} \\ \mathbf{0} & -\boldsymbol{\Omega} \end{bmatrix}, \quad (2)$$

with all blocks being of dimension given by the product of the number of hole and particle states. We define $\mathbf{A} = \boldsymbol{\Delta} + v$, where $\boldsymbol{\Delta}$ is a diagonal matrix of particle-hole excitation energies (provided by a mean field), defining the poles of $\Pi(\omega)$, with $\mathbf{B} = v$ providing the coupling between the excitations and deexcitations via the bare Coulomb interaction, v , in the particle-hole (ph) channel. The diagonal matrix $\boldsymbol{\Omega}$ provides the poles of the RPA dd-response function, $\chi(\omega)$, with the residues defined by the amplitudes of the excitations and deexcitations, \mathbf{X} and \mathbf{Y} , respectively. These form a biorthogonal set of eigenvectors, providing the relations $(\mathbf{X} + \mathbf{Y})^{-1} = (\mathbf{X} - \mathbf{Y})^T$ and $(\mathbf{X} - \mathbf{Y})^{-1} = (\mathbf{X} + \mathbf{Y})^T$. We can expand $\chi(\omega)$ as a Laurent series, with its dynamics fully characterized by the moments of its spectral distribution [40,47], as

$$\eta^{(n)} = (\mathbf{X} + \mathbf{Y})\boldsymbol{\Omega}^n(\mathbf{X} + \mathbf{Y})^T; \quad n \in \mathbb{Z}. \quad (3)$$

The zeroth moment of the distribution $\eta^{(0)}$ characterizes the instantaneous part of the correlated dd response, as $\langle (\hat{c}_i^\dagger \hat{c}_a + \hat{c}_a^\dagger \hat{c}_i)(\hat{c}_j^\dagger \hat{c}_b + \hat{c}_b^\dagger \hat{c}_j) \rangle - \langle \hat{c}_i^\dagger \hat{c}_a + \hat{c}_a^\dagger \hat{c}_i \rangle \langle \hat{c}_j^\dagger \hat{c}_b + \hat{c}_b^\dagger \hat{c}_j \rangle$, summed over the same-spin particle-hole (de)excitations, denoted by indices (a, i) and (b, j) . This describes the correlated contribution to the two-body reduced density matrix, and all resulting static expectation values at the RPA level [48–50]. It is this quantity (through to first order) which we aim to rigorously conserve within a chosen model space with our effective interactions. Crucially, this can be achieved while maintaining *static* renormalized effective interactions in the model space, preserving symmetries, and without changing the reference mean field in the model space.

The structure of the RPA equations imposes a relation between the first two dd-moments [47],

$$\begin{aligned}\eta^{(1)} &= (\mathbf{A} - \mathbf{B}) = \eta^{(0)}(\mathbf{x} - \mathbf{Y})\Omega(\mathbf{X} - \mathbf{Y})^T\eta^{(0)} \\ &= \eta^{(0)}(\mathbf{A} + \mathbf{B})\eta^{(0)}\end{aligned}\quad (4)$$

Inserting the definitions of \mathbf{A} and \mathbf{B} , we find an equation linear in the interaction. This can be analytically inverted to find an interaction kernel that under the RPA gives rise to a desired $\eta^{(0)}$ and $\eta^{(1)}$,

$$v = \frac{1}{2} \left((\eta^{(0)})^{-1} \eta^{(1)} (\eta^{(0)})^{-1} - \mathbf{\Delta} \right). \quad (5)$$

Therefore, by substituting all quantities on the RHS of Eq. (5) for their projection of the full RPA into the chosen model space, an effective static model space interaction can be found, $\mathcal{U}_{\text{mRPA}}$. This ensures that the model space RPA with $v \rightarrow \mathcal{U}_{\text{mRPA}}$ rigorously conserves all full system RPA expectation values derived from $\eta^{(0)}$ and $\eta^{(1)}$ by construction, which includes all instantaneous correlators in the model space. A similar approach to conserve higher-order moments results in equations non-linear in the resulting interaction, and subsequently necessitates a dynamical component to the resulting interaction, as expected to recover the dynamical cRPA limit of the full dd-response [40]. Focusing on conservation of just the first two dd-moments enables a fully static model space screened interaction.

The model space with $\mathcal{U}_{\text{mRPA}}$ can also reproduce the subspace contribution to the RPA correlation energy due to its dependence on $\eta^{(0)}$, as $E_{\text{corr}}^{\text{RPA}} = \frac{1}{2} \text{Tr}[\eta^{(0)}(\mathbf{A} + \mathbf{B}) - \mathbf{A}]$, exploited in the SI (Sec. IV) to demonstrate non-local energetic corrections to the model space. Beyond this, the first two spectral moments of the GW self-energy in the subspace are also exactly described with mRPA interactions, indicating a formal conservation of certain correlated one-body properties [47]. Symmetries, including spin-independence of the resulting effective interactions are also exactly preserved, derived in the SI (Sec. II). These rigorous properties provide a robust footing for use of $\mathcal{U}_{\text{mRPA}}$ in subsequent correlated treatments.

Building $\mathcal{U}_{\text{mRPA}}$ via Eq. (5) required the component of $\eta^{(0)}$ and $\mathbf{\Delta}$ in the subspace. Construction directly from Eqs. (2)–(3) entails a prohibitive $\mathcal{O}(N^6)$ scaling, but this is reduced to an efficient $\mathcal{O}(N^4)$ following the approach detailed in the Supplemental Material [51] (Sec. I). The only constraint on the choice of subspace is that the cluster excitation space is an orthogonal projection of the full system excitation space, i.e., that particle- and holelike character of the subspace orbitals as defined by the reference state is preserved. While this is trivially true where cRPA is valid via a subspace selected from mean-field bands, this is a far looser requirement allowing for a subspace where a nondiagonal $\Pi(\omega)$ couples the

subspace to its environment to be considered. This admits direct mRPA screening of arbitrary (e.g., local atomiclike) subspaces by at most doubling their size by conserving the reference mean-field density matrix over the subspace [58,59], or local spaces formed by localizing hole and virtual bands separately before screening. This direct screening of local subspaces therefore includes screening via long-range low-energy band transitions precluded in traditional cRPA, enabling direct application to *ab initio* quantum embedding clusters.

Interestingly, the resulting $\mathcal{U}_{\text{mRPA}}$ only screens interactions in the ph channel (which is expected to be the dominant long-range contribution to screening), rather than the full four-point interaction. Other approximations (e.g., T matrix for pp diagrams [60–63]) would screen other interaction channels in an analogous formulation, and future work can consider the effect on mRPA interactions from these other channels. It is justified that only the ph channel interaction is screened in mRPA unlike cRPA, since RPA itself is fully determined by this component of the interaction, and mRPA is constructed to describe this RPA physics as opposed to the use of the screening equation [Eq. (1)] in cRPA. This feature of only screening the ph interactions, along with the conservation of the reference density, ensures that the occupied reference band structure (Hartree-Fock or Kohn-Sham) is unchanged with mRPA screened interactions.

Result.—We begin by benchmarking the screening of the low-energy Hartree-Fock orbitals of Benzene (an active space of five hole and five particle states). Benzene has previously been considered a paradigmatic example in this context [25], while also small enough to enable comparison to high-level reference results. In Fig. 1 we show the bare Coulomb, dynamical and static-cRPA, and mRPA subspace interactions traced over all channels. The $\mathcal{U}_{\text{mRPA}}$ is generally less screened than static-cRPA, noting the recent evidence that static-cRPA overscreens interactions [15,28,42]. We can consider the accuracy of resulting subspace observables by comparing to coupled-cluster (CCSD) [64–66]. CCSD encodes the wave function in T amplitudes, and we can consider the projection of the full-system T amplitudes into the active space as an accurate subspace description. This is used to benchmark *subspace-only* CCSD calculations with the different static interactions [67]. We find the mean squared error of the subspace CCSD T_2 amplitudes to be 1.10 for bare subspace interactions, reduced to 0.25 for static-cRPA and only 0.20 for mRPA, indicating that *all* ground-state expectation values within the subspace can be expected to be more faithfully reproduced with mRPA interactions than the alternatives.

While we expect ground states to be particularly faithful given the mRPA conservation of instantaneous correlators, we can also compare the ability of these effective interactions to reproduce the full subspace excitation spectrum. Figure 1 quantifies this via the errors in the subspace RPA

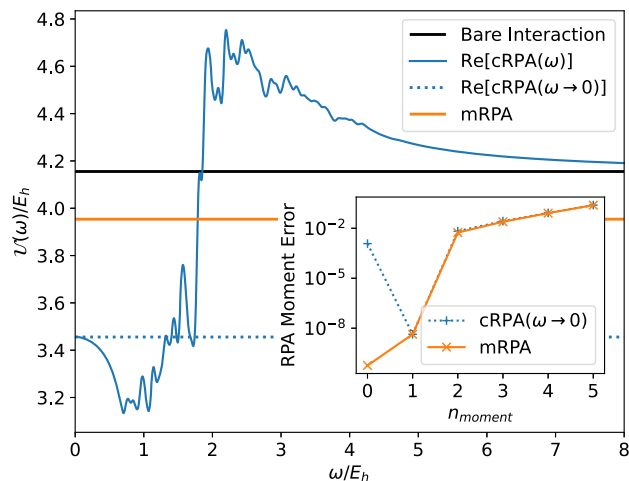


FIG. 1. Trace of the screened and bare interaction, $\mathcal{U}_{pq,pq}$ in a (10,10) CAS space of benzene in a cc-pVDZ basis. Shown are the dynamical cRPA interactions, as well as the widely used static limit, and the static-by-construction mRPA interactions. Inset: Error in the RPA moments as an expansion of the dynamical subspace dd response. The first two mRPA dd moments are exact by construction, yet also exhibit marginally smaller errors for higher moments compared to the static cRPA interaction. Moment error is computed as the mean squared error of $\eta^{(n)}$ over the subspace, normalized by the exact $\|\eta^{(n)}\|_2$ at each order.

moment expansion of Eq. (3) which fully characterizes the dd response. While the first two moments are exact for mRPA by construction (and $\eta^{(1)}$ for static-cRPA), the errors in higher moments are also marginally reduced in their relative error compared to static-cRPA, indicating that the fidelity of the subspace dd response over all frequencies is at least as accurate as static-cRPA.

We now consider the diverse W4-11 test set of 150 molecules, exhibiting a wide range of bonding, radical, and correlated physics [68]. Moving towards direct application of mRPA to quantum embedding methodologies, we consider fragmenting each molecule into individual atoms comprising a minimal set of their intrinsic valence atomic orbitals (IAOs) [69]. These IAO fragments are augmented with an interacting bath of at most the same dimension as the IAO fragment, following the static density matrix embedding (DMET) approach [58,59,70–73]. This defines multiple small atomic subspaces for each molecule, which can be individually solved via CCSD with either bare or mRPA interactions. The resulting subspace CCSD states are recombined to provide a total energy estimator over the subspaces for each molecule (see Refs. [73,74] for more details). These are compared to the energy of the exact full-system CCSD projected into these subspaces. This discrepancy quantifies the ability of the mRPA to account for relaxation of these embedded atomic descriptions due to the neglected interactions with the rest of the molecule.

Figure 2 shows this error aggregated over the test set in increasingly large basis sets, where screening of these

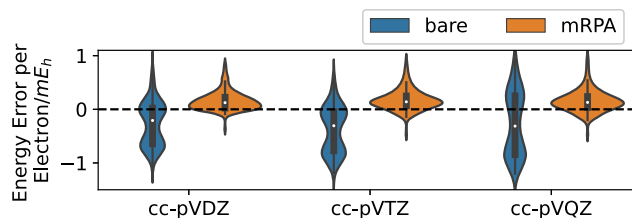


FIG. 2. Distribution of energy errors in atomically fragmented DMET-CCSD with bare or mRPA interactions across the W4-11 test set of 150 molecules, in increasingly large basis sets. Errors are computed comparing to the full-system CCSD of each molecule projected into each subspace.

low-energy subspaces by higher-energy scattering dominates. The mRPA interactions screen the fragments defined by the embedding, resulting in a substantial $\sim 66\%$ reduction in both the mean absolute error and standard deviation of the energy error across the dataset. This consistent reduction in error across larger basis sets points for these diverse systems attests to the broad applicability of the mRPA interactions for correlated systems. We note that cRPA cannot be easily compared in this context, due to the difficulties in directly screening subspaces that are not mean-field orbitals, as discussed previously.

Finally, we consider the application of mRPA to extended systems where long-range collective plasmons strongly renormalize local properties, which are difficult to describe in a local subspace [25,75]. Furthermore, we demonstrate systematic improvability of this screened local subspace. This is achieved in a consistent framework via extending the bath space, formally including additional states which exactly minimize the error of the subspace RPA $\eta^{(0)}$ with bare interactions, thereby spanning physics at longer length scales in the model subspaces. The algebraic construction of these additional bath states relies on evaluation of the same quantities as the mRPA interactions, and systematically enlarges the local correlated subspaces in an optimal way to completeness, with details in the Supplemental Material [51] (Sec. III). This approach is inspired by the unscreened perturbative bath expansion of Ref. [73], but here adapted for a screened embedding.

We converge semimetallic graphene sheets with a fully *ab initio* CCSD description, embedding atomic fragments and systematically enlarging the bath space for each fragment. On enlarging, the bath interactions provide increased screening of the fragments explicitly, and the mRPA static screening is correspondingly reduced in a fashion that precludes double counting of the fragment screening and naturally converges to an in-method (CCSD) exact limit. Figure 3 shows fully *ab initio* two-body instantaneous charge and spin fluctuations in the local atomic $2p_z$ space, on top of a symmetry-preserving Hartree-Fock reference [74,76]. The correlated treatment quantitatively changes these two-body correlators, but bare subspace interactions overestimate the magnitude of the changes

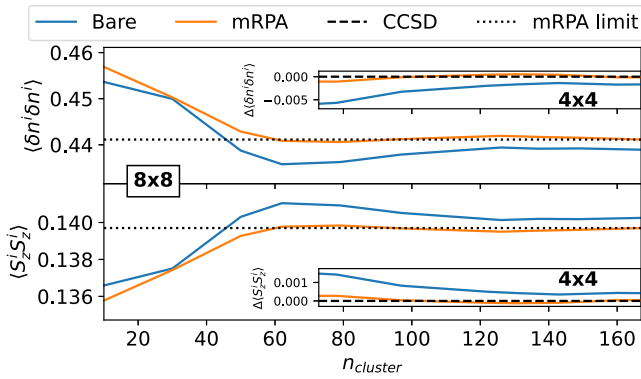


FIG. 3. Convergence of the CCSD local $2p_z$ -orbital charge (top) and spin (bottom) two-body fluctuations in 8×8 graphene sheets with increasing size of embedded cluster, for both bare Coulomb and mRPA cluster interactions. Inset: Error in these two-body correlators in 4×4 \mathbf{k} -point meshes, where comparison to exact CCSD is possible.

from mean field. Importantly, the bias in these correlators with the bare interactions appears unable to be compensated for with increasing bath, indicating the importance of coupling to truly long-range $\mathbf{q} \rightarrow 0$ plasmonic modes for an appropriate relaxation of these local properties, impractical in a local embedding with bare interactions.

In contrast, the mRPA screened interactions fold in this coupling, resulting in a rapid and stable convergence with increasing bath size, corroborated with smaller 4×4 \mathbf{k} -point meshes where comparison to the full system CCSD result is possible and the same qualitative behavior is observed. While $\mathcal{U}_{\text{mRPA}}$ is static, it nevertheless integrates over all RPA diagrams, including plasmonic contributions required to appropriately relax the subspace. This even impacts on the convergence of magnetic correlators in the subspace, despite not being described in the $\eta^{(0)}$ description of RPA density fluctuations. The results indicate that the plasmonic coupling therefore suppresses the tendency towards formation of atomic magnetic moments in graphene. In the Supplemental Material [51] (Sec. IV) we also demonstrate improvements in *nonlocal* magnetic fluctuations as well as energetics in this system, and the insensitivity of these results to choice of underlying reference mean-field theory.

In summary, the developed “mRPA” efficiently integrates over all external RPA diagrams to provide a manifestly static effective interaction for low energy or local models, conserving all instantaneous RPA correlators in a chosen subspace by construction. For multimethod work flows, we show this provides a systematic and principled route for the inclusion of long-range and high-energy screening in a local correlation framework. This also opens opportunities in the push for fully improvable and nonempirical quantum embedding, with reliable convergence in extended systems coupled to long-range coherent quasiparticles.

All calculations were performed and can be reproduced with the VAYESTA quantum embedding code [77].

The authors gratefully acknowledge support from the European Union’s Horizon 2020 research and innovation programme under Grant Agreement No. 759063. We are grateful to the UK Materials and Molecular Modelling Hub for computational resources, which is partially funded by EPSRC (EP/P020194/1 and EP/T022213/1).

*charles.j.scott@kcl.ac.uk

†george.booth@kcl.ac.uk

- [1] J. Hubbard and B. H. Flowers, *Proc. Roy. Soc. London A* **277**, 237 (1964).
- [2] F. Jørgensen, *Mol. Phys.* **29**, 1137 (1975).
- [3] I. Shavitt and L. T. Redmon, *J. Chem. Phys.* **73**, 5711 (2008).
- [4] P. Löwdin, *J. Chem. Phys.* **19**, 1396 (2004).
- [5] H. Ma, N. Sheng, M. Govoni, and G. Galli, *J. Chem. Theory Comput.* **17**, 2116 (2021).
- [6] H. Zheng, H. J. Changlani, K. T. Williams, B. Busemeyer, and L. K. Wagner, *Front. Phys.* **6**, 43 (2018).
- [7] Y. Chang and L. K. Wagner, Learning emergent models from *ab initio* many-body calculations (2023), arXiv:2302.02899 [cond-mat.str-el].
- [8] G. Rohringer, H. Hafermann, A. Toschi, A. A. Katanin, A. E. Antipov, M. I. Katsnelson, A. I. Lichtenstein, A. N. Rubtsov, and K. Held, *Rev. Mod. Phys.* **90**, 025003 (2018).
- [9] G. Kotliar, S. Y. Savrasov, K. Haule, V. S. Oudovenko, O. Parcollet, and C. A. Marianetti, *Rev. Mod. Phys.* **78**, 865 (2006).
- [10] Q. Sun and G. K.-L. Chan, *Acc. Chem. Res.* **49**, 2705 (2016).
- [11] M. Ditte, M. Barborini, L. M. Sandonas, and A. Tkatchenko, *Phys. Rev. Lett.* **131**, 228001 (2023).
- [12] Y. Nomura, M. Kaltak, K. Nakamura, C. Taranto, S. Sakai, A. Toschi, R. Arita, K. Held, G. Kresse, and M. Imada, *Phys. Rev. B* **86**, 085117 (2012).
- [13] E. Şaşıoğlu, C. Friedrich, and S. Blügel, *Phys. Rev. B* **83**, 121101(R) (2011).
- [14] M. Springer and F. Aryasetiawan, *Phys. Rev. B* **57**, 4364 (1998).
- [15] M. Kinza and C. Honerkamp, *Phys. Rev. B* **92**, 045113 (2015).
- [16] X.-J. Han, P. Werner, and C. Honerkamp, *Phys. Rev. B* **103**, 125130 (2021).
- [17] F. Aryasetiawan, J. M. Tomczak, T. Miyake, and R. Sakuma, *Phys. Rev. Lett.* **102**, 176402 (2009).
- [18] J. W. Park, R. Al-Saadon, M. K. MacLeod, T. Shiozaki, and B. Vlasisavljevich, *Chem. Rev.* **120**, 5878 (2020).
- [19] V. Katukuri, N. Bogdanov, O. Weser, J. Brink, and A. Alavi, *Phys. Rev. B* **102**, 241112 (2020).
- [20] G. P. Chen, V. K. Voora, M. M. Agee, S. G. Balasubramani, and F. Furche, *Annu. Rev. Phys. Chem.* **68**, 421 (2017).
- [21] M. W. Jørgensen and S. P. A. Sauer, *J. Chem. Phys.* **152**, 234101 (2020).
- [22] D. Bohm and D. Pines, *Phys. Rev.* **92**, 609 (1953).
- [23] M. Gell-Mann and K. A. Brueckner, *Phys. Rev.* **106**, 364 (1957).
- [24] M. Shishkin and G. Kresse, *Phys. Rev. B* **75**, 235102 (2007).

- [25] E. G. C. P. van Loon, M. Rösner, M. I. Katsnelson, and T. O. Wehling, *Phys. Rev. B* **104**, 045134 (2021).
- [26] F. Aryasetiawan, M. Imada, A. Georges, G. Kotliar, S. Biermann, and A. I. Lichtenstein, *Phys. Rev. B* **70**, 195104 (2004).
- [27] T. Miyake and F. Aryasetiawan, *Phys. Rev. B* **77**, 085122 (2008).
- [28] H. Shinaoka, M. Troyer, and P. Werner, *Phys. Rev. B* **91**, 245156 (2015).
- [29] L. Vaugier, H. Jiang, and S. Biermann, *Phys. Rev. B* **86**, 165105 (2012).
- [30] A. Hausoel, M. Karolak, E. Şaşıoğlu, A. Lichtenstein, K. Held, A. Katanin, A. Toschi, and G. Sangiovanni, *Nat. Commun.* **8**, 16062 (2017).
- [31] R. Sakuma and F. Aryasetiawan, *Phys. Rev. B* **87**, 165118 (2013).
- [32] E. G. C. P. van Loon, M. Rösner, G. Schönhoff, M. I. Katsnelson, and T. O. Wehling, *npj Quantum Mater.* **3**, 32 (2018).
- [33] P. Werner, R. Sakuma, F. Nilsson, and F. Aryasetiawan, *Phys. Rev. B* **91**, 125142 (2015).
- [34] S. W. Jang, H. Sakakibara, H. Kino, T. Kotani, K. Kuroki, and M. J. Han, *Sci. Rep.* **6**, 33397 (2016).
- [35] J. Chen, A. J. Millis, and C. A. Marianetti, *Phys. Rev. B* **91**, 241111(R) (2015).
- [36] Y. Nomura, M. Hirayama, T. Tadano, Y. Yoshimoto, K. Nakamura, and R. Arita, *Phys. Rev. B* **100**, 205138 (2019).
- [37] C. Martins, M. Aichhorn, L. Vaugier, and S. Biermann, *Phys. Rev. Lett.* **107**, 266404 (2011).
- [38] B.-C. Shih, Y. Zhang, W. Zhang, and P. Zhang, *Phys. Rev. B* **85**, 045132 (2012).
- [39] K. Yoshimi, T. Misawa, T. Tsumuraya, and H. Seo, *Phys. Rev. Lett.* **131**, 036401 (2023).
- [40] C. J. C. Scott and G. H. Booth, *Phys. Rev. B* **104**, 245114 (2021).
- [41] N. Sheng, C. Vorwerk, M. Govoni, and G. Galli, *J. Chem. Theory Comput.* **18**, 3512 (2022).
- [42] C. Honerkamp, H. Shinaoka, F. F. Assaad, and P. Werner, *Phys. Rev. B* **98**, 235151 (2018).
- [43] M. Casula, P. Werner, L. Vaugier, F. Aryasetiawan, T. Miyake, A. J. Millis, and S. Biermann, *Phys. Rev. Lett.* **109**, 126408 (2012).
- [44] T. Miyake, F. Aryasetiawan, and M. Imada, *Phys. Rev. B* **80**, 155134 (2009).
- [45] F. Aryasetiawan, T. Miyake, and R. Sakuma, in *The LDA + DMFT Approach to Strongly Correlated Materials, 2011 Reihe Modeling and Simulation*, edited by E. Pavarini, E. Koch, D. Vollhardt, and A. Lichtenstein (Verlag des Forschungszentrum Jülich, 2011), Vol. 1, Chap. 7.
- [46] M. E. Casida, in *Recent Advances In Density Functional Methods: (Part I)* (World Scientific, Singapore, 1995), pp. 155–192.
- [47] C. J. C. Scott, O. J. Backhouse, and G. H. Booth, *J. Chem. Phys.* **158**, 124102 (2023).
- [48] J. Toulouse, I. C. Gerber, G. Jansen, A. Savin, and J. G. Ángyán, *Phys. Rev. Lett.* **102**, 096404 (2009).
- [49] J. Toulouse, W. Zhu, J. G. Ángyán, and A. Savin, *Phys. Rev. A* **82**, 032502 (2010).
- [50] J. G. Ángyán, R.-F. Liu, J. Toulouse, and G. Jansen, *J. Chem. Theory Comput.* **7**, 3116 (2011).
- [51] See Supplemental Material at <http://link.aps.org/supplemental/10.1103/PhysRevLett.132.076401> for details of the efficient algorithm for RPA moment construction and their spin independence, as well as construction of RPA-derived fermionic bath orbitals and the construction of nonlocal expectation values with the screened interaction, which includes Refs. [52–57].
- [52] H. Eshuis, J. Yarkony, and F. Furche, *J. Chem. Phys.* **132**, 234114 (2010).
- [53] N. Hale, N. J. Higham, and L. N. Trefethen, *SIAM J. Numer. Anal.* **46**, 2505 (2008).
- [54] C.-N. Yeh, S. Isakov, D. Zgid, and E. Gull, *Phys. Rev. B* **106**, 235104 (2022).
- [55] T. Zhu and G. K.-L. Chan, *J. Chem. Theory Comput.* **17**, 727 (2021).
- [56] D. Kosov, *Chem. Phys. Lett.* **690**, 20 (2017).
- [57] J. McClain, Q. Sun, G. K.-L. Chan, and T. C. Berkelbach, *J. Chem. Theory Comput.* **13**, 1209 (2017).
- [58] G. Knizia and G. K.-L. Chan, *Phys. Rev. Lett.* **109**, 186404 (2012).
- [59] S. Sekaran, O. Bindech, and E. Fromager, *J. Chem. Phys.* **159**, 034107 (2023).
- [60] N. Bickers and D. Scalapino, *Ann. Phys. (N.Y.)* **193**, 206 (1989).
- [61] H. van Aggelen, Y. Yang, and W. Yang, *Phys. Rev. A* **88**, 030501(R) (2013).
- [62] J. Gukelberger, L. Huang, and P. Werner, *Phys. Rev. B* **91**, 235114 (2015).
- [63] M. Springer, F. Aryasetiawan, and K. Karlsson, *Phys. Rev. Lett.* **80**, 2389 (1998).
- [64] Q. Sun, T. C. Berkelbach, N. S. Blunt, G. H. Booth, S. Guo, Z. Li, J. Liu, J. D. McClain, E. R. Sayfutyarova, S. Sharma, S. Wouters, and G. K.-L. Chan, *WIREs Comput. Mol. Sci.* **8**, e1340 (2018).
- [65] Q. Sun *et al.*, *J. Chem. Phys.* **153**, 024109 (2020).
- [66] R. J. Bartlett and M. Musiał, *Rev. Mod. Phys.* **79**, 291 (2007).
- [67] Coupled-cluster is defined in terms of the Fock matrix and fluctuation potential. The virtual-virtual block of the Fock matrix is shifted by $\Delta f_{ab} = \sum_{i \in \text{occ}} (ia|bi) - \mathcal{U}_{ia,ib}$ due to the screened ph mRPA interactions, but other blocks are unchanged ensuring the reference-independence of mRPA.
- [68] A. Karton, S. Daon, and J. M. Martin, *Chem. Phys. Lett.* **510**, 165 (2011).
- [69] G. Knizia, *J. Chem. Theory Comput.* **9**, 4834 (2013).
- [70] G. Knizia and G. K.-L. Chan, *J. Chem. Theory Comput.* **9**, 1428 (2013).
- [71] S. Wouters, C. A. Jiménez-Hoyos, Q. Sun, and G. K.-L. Chan, *J. Chem. Theory Comput.* **12**, 2706 (2016).
- [72] Z.-H. Cui, T. Zhu, and G. K.-L. Chan, *J. Chem. Theory Comput.* **16**, 119 (2020).
- [73] M. Nusspickel and G. H. Booth, *Phys. Rev. X* **12**, 011046 (2022).
- [74] M. Nusspickel, B. Ibrahim, and G. H. Booth, *J. Chem. Theory Comput.* **19**, 2769 (2023).
- [75] T. O. Wehling, E. Şaşıoğlu, C. Friedrich, A. I. Lichtenstein, M. I. Katsnelson, and S. Blügel, *Phys. Rev. Lett.* **106**, 236805 (2011).
- [76] P. Pokhilko and D. Zgid, *J. Chem. Phys.* **155**, 024101 (2021).
- [77] VAYESTA code available at <https://github.com/BoothGroup/Vayesta>.